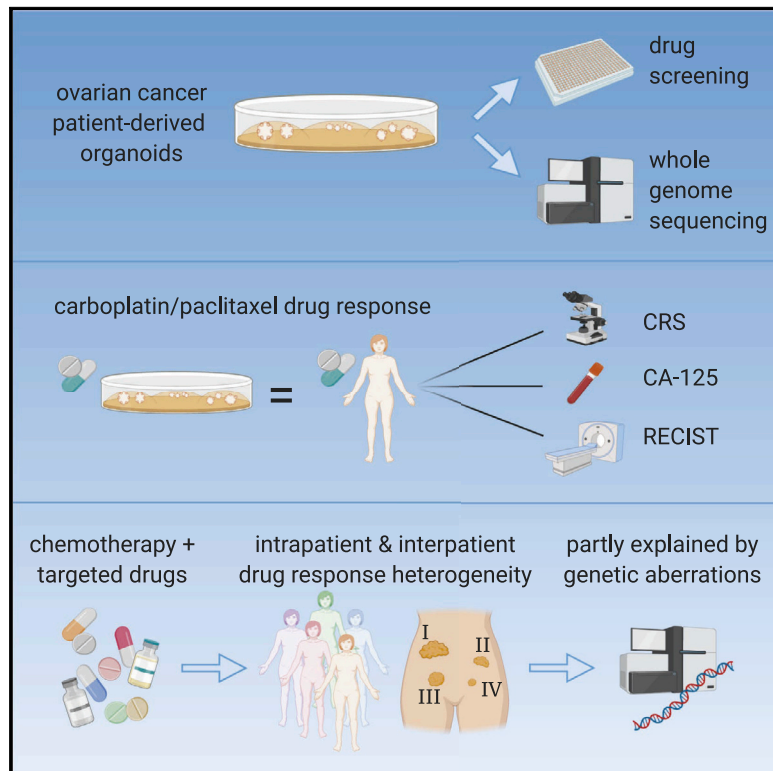Article

Patient-Derived Ovarian Cancer Organoids Mimic Clinical Response and Exhibit Heterogeneous Inter- and Intrapatient Drug Responses

Graphical Abstract

Authors

Chris Jenske de Witte,
Jose Espejo Valle-Inclan, Nizar Hami, ...,
Ronald Peter Zweemer,
Petronella Oda Witteveen, Ellen Stelloo

Correspondence

e.stelloo@umcutrecht.nl

In Brief

De Witte et al. employ patient-derived organoids (PDOs) for *ex vivo* drug screening. Ovarian cancer (OC) PDOs often recapitulate patient drug response to first-line chemotherapy. In addition, OC PDOs display inter- and intrapatient drug response heterogeneity to chemotherapy and targeted drugs, which can be partly explained by genetic aberrations.

Highlights

- Patient-derived organoids (PDOs) as drug screening models in ovarian cancer (OC)

- OC PDOs often recapitulate patient response to carboplatin and paclitaxel treatment

- OC PDOs display inter- and intrapatient drug response heterogeneity

- OC PDO drug response heterogeneity can be partly explained by genetic aberrations

CellPress

Cell Reports

Article

Patient-Derived Ovarian Cancer Organoids Mimic Clinical Response and Exhibit Heterogeneous Inter- and Intrapatient Drug Responses

Chris Jenske de Witte,[1,2] Jose Espejo Valle-Inclan,[1,2] Nizar Hami,[2,3] Kadi Lõhmussaar,[2,4] Oded Kopper,[2,4] Celien Philomena Henrieke Vreuls,[5] Geertruida Nellie Jonges,[5] Paul van Diest,[5] Luan Nguyen,[1,2] Hans Clevers,[2,4] Wigard Pieter Kloosterman,[1] Edwin Cuppen,[1,2,6] Hugo Johannes Gerhardus Snippert,[2,3] Ronald Peter Zweemer,[7] Petronella Oda Witteveen,[8,9] and Ellen Stelloo[1,2,9,10,*]

[1]Genetics, Center for Molecular Medicine, University Medical Center Utrecht, Utrecht University, Universiteitsweg 100, 3584 CG Utrecht, the Netherlands
[2]Oncode Institute, Jaarbeursplein 6, 3521 AL Utrecht, the Netherlands
[3]Molecular Cancer Research, Center for Molecular Medicine, University Medical Center Utrecht, Utrecht University, Universiteitsweg 100, 3584 CG Utrecht, the Netherlands
[4]Hubrecht Institute, Royal Netherlands Academy of Arts and Sciences and University Medical Center Utrecht, Uppsalalaan 8, 3584 CT Utrecht, the Netherlands
[5]Department of Pathology, University Medical Center Utrecht, Utrecht University, Heidelberglaan 100, 3584 CX Utrecht, the Netherlands
[6]Hartwig Medical Foundation, Science Park 408, 1098 XH Amsterdam, the Netherlands
[7]Division of Imaging and Oncology, Department of Gynecological Oncology, University Medical Center Utrecht, Utrecht University, Heidelberglaan 100, 3584 CX Utrecht, the Netherlands
[8]Department of Medical Oncology, Cancer Center, University Medical Center Utrecht, Utrecht University, Heidelberglaan 100, 3584 CX Utrecht, the Netherlands
[9]Senior author
[10]Lead Contact
*Correspondence: e.stelloo@umcutrecht.nl
https://doi.org/10.1016/j.celrep.2020.107762

SUMMARY

There remains an unmet need for preclinical models to enable personalized therapy for ovarian cancer (OC) patients. Here we evaluate the capacity of patient-derived organoids (PDOs) to predict clinical drug response and functional consequences of tumor heterogeneity. We included 36 whole-genome-characterized PDOs from 23 OC patients with known clinical histories. OC PDOs maintain the genomic features of the original tumor lesion and recapitulate patient response to neoadjuvant carboplatin/paclitaxel combination treatment. PDOs display inter- and intrapatient drug response heterogeneity to chemotherapy and targeted drugs, which can be partially explained by genetic aberrations. PDO drug screening identifies high responsiveness to at least one drug for 88% of patients. PDOs are valuable preclinical models that can provide insights into drug response for individual patients with OC, complementary to genetic testing. Generating PDOs of multiple tumor locations can improve clinical decision making and increase our knowledge of genetic and drug response heterogeneity.

INTRODUCTION

Epithelial ovarian cancer (OC) is characterized by development of chemotherapy resistance and poor survival. Overall survival for patients with OC has only slightly improved over the past decades despite developments in the field, such as optimized surgical tumor resection, administration of (hyperthermic) intra-peritoneal chemotherapy, and introduction of targeted treatments such as poly ADP ribose polymerase (PARP) inhibitors (Timmermans et al., 2018). Although most patients with OC respond well to initial treatment, the majority will develop recurrent disease within the first 2 years and become resistant to chemotherapy. In the setting of recurrent disease, a wide range

of chemotherapeutic and targeted drugs is available. PARP inhibitors are indicated for patients who experienced a complete or partial response to previous platinum treatment irrespective of BRCA1/2 mutation status (Mirza et al., 2016). Still, BRCA1/2 mutation carriers experience more benefit from PARP inhibition compared with patients with homologous recombination (HR)-proficient tumors (Mirza et al., 2016). However, for the majority of relapsed patients and drugs, no genetic markers are available to predict response. These patients might benefit from patient-derived model systems that can be employed to test response to drugs prior to treatment in the clinic.

Traditionally, OC drug response has been studied in 2D cell lines and xenografts. 2D cell lines are a relatively cheap and

quick model system suitable for high-throughput drug screening, whereas patient-derived xenografts offer the potential to study tumor drug response in a living organism but are not suitable for high-throughput drug screening experiments (Bleijs et al., 2019). In the past decade, patient-derived organoids (PDOs) have been established (Sato et al., 2011), a 3D cell culture model system that maintains the cellular heterogeneity of healthy tissues and tumors. Recently, PDOs of OC were established that represent the genomic features of the original tumors (Hill et al., 2018; Jabs et al., 2017; Kopper et al., 2019). Furthermore, a drug screening comparison between 2D cultures and PDOs of OC revealed that cytostatic drug efficacy is dependent on the employed culture system; PDO drug responses correlate better with genomic aberrations compared with 2D cell cultures (Jabs et al., 2017). To employ the organoid system to guide treatment choice in the clinic, it is vital that a correlation between PDO drug response and clinical drug response is established. To this extent, prospective clinical trials have been performed with PDOs of patients with colorectal cancer, where *in vitro* drug screening recapitulated patient response to chemotherapy and targeted drugs (Ooft et al., 2019; Vlachogiannis et al., 2018). For OC, we and others previously provided anecdotal evidence a correlation between clinical and PDO drug response (Hill et al., 2018; Kopper et al., 2019; Swan et al., 2018), but direct comparisons are still limited.

When predicting treatment response, genetic heterogeneity should be considered. Epithelial OC, especially the high-grade serous subtype, is a heterogeneous disease with widespread inter- and intrapatient genetic heterogeneity (Hoogstraat et al., 2014; Patch et al., 2015). A virtue of the PDO model system is the possibility to study genetic and phenotypic tumor heterogeneity (Roerink et al., 2018).

In this study, we systematically assessed whether the *in vitro* drug response of OC PDOs correlates with patients' clinical response to chemotherapeutic agents. We studied inter- and intrapatient drug response heterogeneity to a wide range of chemotherapeutic agents as well as targeted drugs and linked differential drug response to genetic variation.

RESULTS

PDOs Can Be Established (Rapidly) from Different OC Subtypes

In total, we included 36 PDOs (29 of which have been established previously; Kopper et al., 2019) derived from 23 patients with different histological subtypes of OC who underwent primary or interval debulking surgery or ascites drainage (Table S1). PDO sample names are informative of the histological subtype as well as the patient (first number) and tumor location (second number). We have demonstrated previously that PDOs are largely similar to the carcinoma fields within their matching tumor, based on histopathological assessment (Kopper et al., 2019). The majority of PDOs in our biobank were thoroughly characterized by whole-genome sequencing and histopathological examination and biobanked prior to drug testing to establish a reliable platform. This resulted in a considerable length of time from PDO establishment to drug screening. However, to incorporate PDO-based drug response prediction in clinical care,
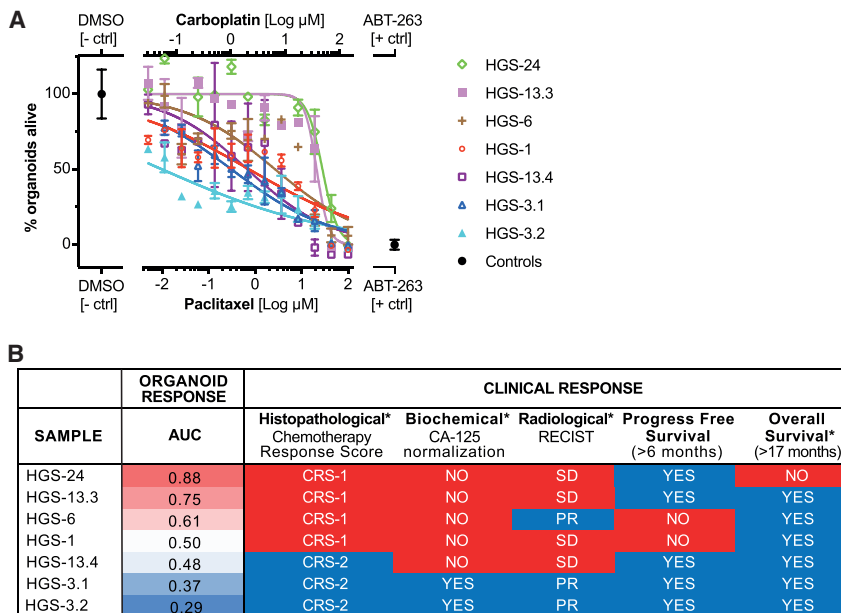
PDO establishment and screening must be executed within a short time span. As a pilot experiment, we successfully established and rapidly screened organoids from a patient with recurrent disease (HG-26; Figures S1A–S1C). Within 20 days of tumor collection, the response to six therapies became available.

PDOs Retained the Genomic Features of the Original Tumor Lesion

We characterized 36 organoids, 30 matching tumors, and 31 germline samples by whole-genome sequencing to an average coverage of 32×. Passage numbers at which PDOs were sequenced are provided in Table S1. First we compared the genomic profiles of PDOs and the tumors from which they were derived. An average of 8,290 and 10,358 SNVs were identified in the parental tumor specimen and their matched PDO, respectively. On average, 67% of variants were shared between the tumor and PDO, and 6% of the SNVs were unique to the tumor and 27% to the PDO (Figure S2A). Assessment of copy number alterations (CNAs) demonstrated comparable copy number states in the majority of pairs (Figures S2B and S2C). HGS-3.1, LGS-2.2, and MC-2.1 presented with a much higher number of SNVs than their matched tumor specimens and considerable CNA dissimilarities within PDO-tumor pairs. These exceptions are likely due to a high degree of normal cell contamination in the tumor samples, which was confirmed by PURPLE, a purity ploidy estimator (Table S7; Cameron et al., 2019). In general, based on PURPLE tumor content estimates (Table S7), PDOs are enriched for tumor cells, whereas tumor samples are heterogeneous, representing a mix of tumor cells and normal cells. For tumor samples with tumor content, PDOs retained the genomic features of the original tumor lesions.

PDO Drug Response Correlates with Patients' Clinical Response

Next we evaluated the potential of PDOs to reflect patients' drug response to chemotherapy. For this, we selected all PDOs that were derived from interval debulking surgery from patients with HGS OC with known clinical histories (Tables S1 [clinical comparison] and S2). Seven PDOs (derived from five patients) were exposed to carboplatin and paclitaxel combination treatment *in vitro*, and we could directly compare their response with the patients' clinical response. The related samples HGS-3.1 and HGS-3.2 were most responsive to carboplatin and paclitaxel combination treatment (area under the curve [AUC] = 0.37 and 0.29, respectively), whereas HGS-24 was the least responsive (AUC = 0.88) (Figure 1). These PDO drug responses showed a statistically significant correlation (p < 0.01) with clinical response, as measured by histopathological (chemotherapy response score [CRS]), biochemical (normalization of the serum biomarker CA-125), and radiological (RECIST) responses (Figure 1; Figures S1D–S1H). The derivation of organoids upon interval debulking was restricted to CRS1- and CRS2-scored samples, a high-risk subgroup of patients, because CRS3-scored samples do not have macroscopic tumor lesions from which the pathologist can provide tissue for organoid derivation. PDOs derived from tumor locations with no or a minimal histopathological response (CRS = 1) were less responsive to carboplatin and paclitaxel combination treatment compared with

A

B

SAMPLE	ORGANOID RESPONSE	CLINICAL RESPONSE				
	AUC	Histopathological* Chemotherapy Response Score	Biochemical* CA-125 normalization	Radiological* RECIST	Progress Free Survival (>6 months)	Overall Survival* (>17 months)
HGS-24	0.88	CRS-1	NO	SD	YES	NO
HGS-13.3	0.75	CRS-1	NO	SD	YES	YES
HGS-6	0.61	CRS-1	NO	PR	NO	YES
HGS-1	0.50	CRS-1	NO	SD	NO	YES
HGS-13.4	0.48	CRS-2	NO	SD	YES	YES
HGS-3.1	0.37	CRS-2	YES	PR	YES	YES
HGS-3.2	0.29	CRS-2	YES	PR	YES	YES

Figure 1. OC PDO Drug Response Correlates with Clinical Drug Response

(A) Drug dose-response curves of OC PDOs for carboplatin and paclitaxel combination. Dose-response curves are normalized to positive (navitoclax, ABT-263) and negative controls (DMSO). Top x axis: carboplatin drug concentrations; bottom x axis, paclitaxel drug concentrations. Each drug concentration was tested twice (technical replicate). Data points and error bars represent the mean and standard deviation of one technical replicate. Non-linear regression analysis: log(inhibitor) versus response fit. Red, clinically resistant; blue, clinically sensitive.

(B) Overview of PDO drug response (area under the curve [AUC]) versus all clinical response measures, ordered from low-responsive to high-responsive based on AUC values. Histopathological tumor response: CRS1, no or minimal response; CRS2, appreciable response; $p = 5.821e-05$. Biochemical response: no normalization (<35 kU/L) of serum CA-125 during primary treatment versus normalization; $p = 0.0004$. Radiological response: stable disease versus partial response (PR) according to RECIST criteria; $p = 0.0092$.

See also Figures S1D–S1H. *$p < 0.01$; statistically significant difference between the clinically sensitive and resistant groups according to Wilcoxon signed-rank test corrected for multiple testing.

PDOs derived from tumor locations with an appreciable pathological response (CRS = 2) ($p = 5.821e-05$, Wilcoxon signed-rank test) (Böhm et al., 2015). Biochemically, clinical drug response is measured according to the response criteria and timing of normalization of CA-125 (Eisenhauer et al., 2009; Rustin et al., 2004). Even though all patients exhibited CA-125 response during primary treatment, PDOs derived from patients who did not reach CA-125 normalization during primary treatment were less responsive to the chemotherapeutic agents compared with PDOs from a patient in whom CA-125 levels normalized (<35 kU/L, $p = 0.0004$). Radiological response was assessed according to the RECIST criteria (version 1.1) (Eisenhauer et al., 2009), comparing imaging data at initiation of chemotherapy with imaging data prior to interval debulking based on computed tomography (CT) scanning. PDOs derived from patients with RE-CIST stable disease were less responsive to carboplatin and paclitaxel combination treatment compared with PDOs from patients with a RECIST partial response ($p = 0.0092$). To compare long-term clinical response with PDO response, recurrence and survival were assessed. All patients experienced recurrent disease within 4–14 months after the last primary treatment, and 6-month progression-free survival (PFS) did not correlate with PDO drug response. After 17 months, 50% of patients with FIGO stage IV HGS OC are still alive (Table S2); only one of five patients (HGS-24) in our cohort lived less than 17 months, and this PDO exhibited the least responsiveness to carboplatin and paclitaxel combination treatment.

PDOs Exhibit Interpatient Drug Response Heterogeneity that Correlates Partially with Their Genetic Makeup

Next we investigated the response of all PDOs (n = 36) to a broader range of drugs and drug combinations (3–17 per PDO,

on average 13; Table S3), including chemotherapeutic agents and targeted drugs. Drugs were selected based on clinical practice or evaluation in clinical trials for OC or solid tumors in general. Drug response experiments were performed in technical replicates, and replicate AUC values highly correlated ($R^2 = 0.87$) (Figure S3A). Passage numbers at which PDOs were screened for drug response are provided in Table S1. PDOs were classified into a low-response subgroup when the drug concentration that reduced viability of less than 50% of cells (IC$_{50}$ value) was higher than the concentration achievable in patient plasma (concentration steady state/maximum concentration $Css/Cmax$]; Table S3; Schumacher et al., 2019; Yan et al., 2018) and a high-response subgroup when the IC$_{50}$ value was lower than the $Css/Cmax$.

Divergent responses were observed to the chemotherapeutic drugs carboplatin (platinum/alkylating agent), paclitaxel (taxane/antimicrotubule agent), and gemcitabine (pyrimidine antagonist) (Figures 2A–2C; Table S3). A minority of PDOs was classified into the high-response subgroup of carboplatin (7 of 31, 23%) and paclitaxel monotherapy (5 of 31, 16%), whereas most PDOs (29 of 35, 83%) were in the high-response subgroup of gemcitabine. Response also correlated with OC histological subtype; all LGS samples showed low responsiveness to paclitaxel and carboplatin monotherapy (except for the response to carboplatin in LGS-3.1), whereas high responsiveness was restricted to HG(S) samples. For certain PDOs, combination treatment with two chemotherapeutic drugs had a greater effect on viability (lower IC$_{50}$ values) than the drugs' individual effects (Table S3), indicating an additive or synergistic effect of the combined drugs. Our results, for example, showed that carboplatin and paclitaxel treatment alone had a minimal effect on LGS-3.1, with an IC$_{50}$ value of 1.46 and more than 2.5 log μM, respectively, whereas
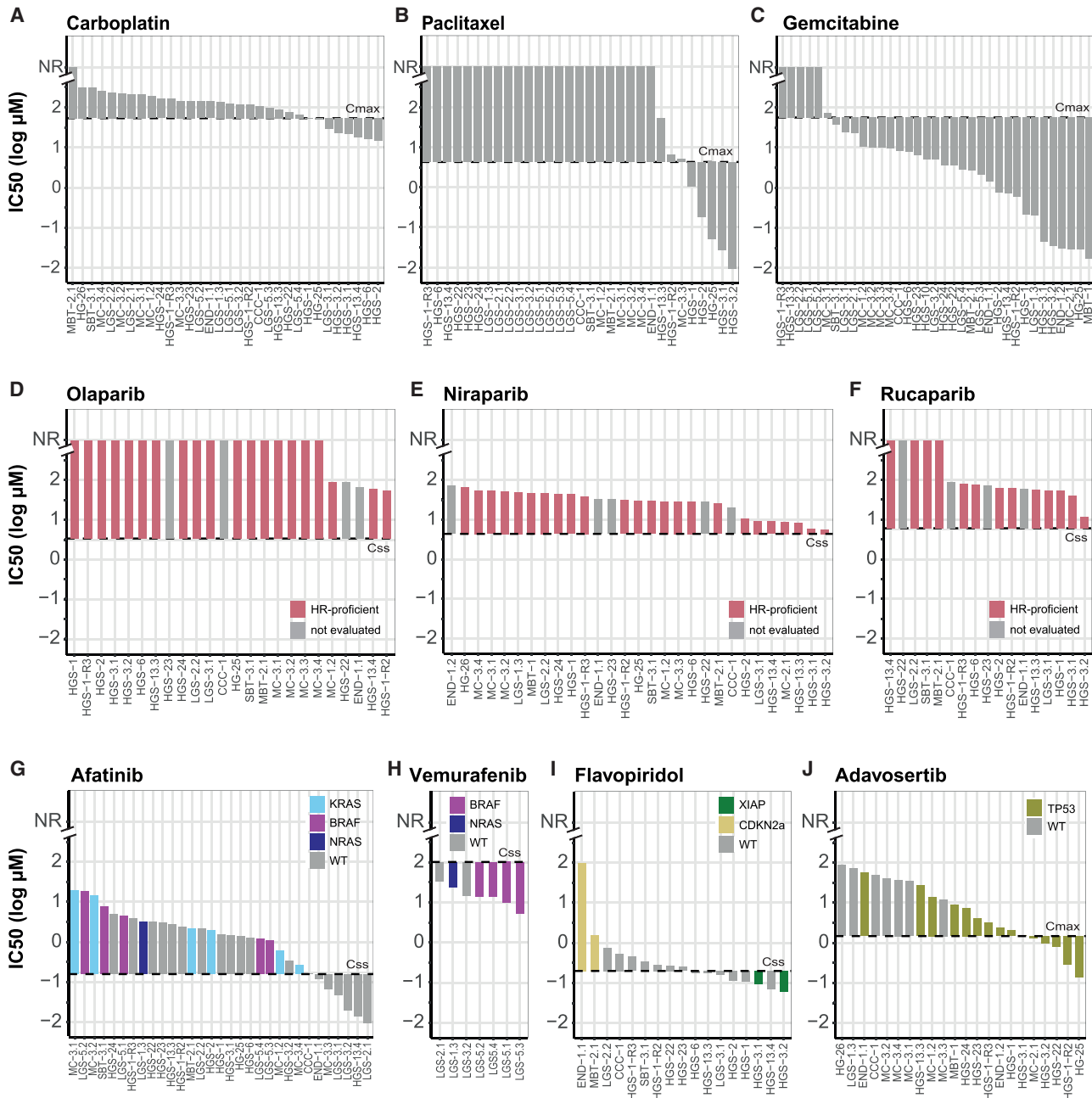
**Figure 2. OC PDOs Exhibit Interpatient Heterogeneity in Response to Chemotherapy and Targeted Drugs**

Waterfall plots with IC_{50} values (extracted from dose-response curves) of OC PDOs for chemotherapeutic agents and targeted drugs. The steady-state (Css) or maximum ($Cmax$) *in vivo* plasma concentrations are indicated by the dotted line (Table S3). Bars above the dotted line represent low-response samples, and bars below the dotted line represent high-response samples.

(A–C) Response to the chemotherapeutic agents carboplatin (A), paclitaxel (B), and gemcitabine (C).

(D–F) Response to the PARP inhibitors olaparib (D), niraparib (E), and rucaparib (F). All PDOs were classified as low- responsive to the PARP inhibitors, which correlated with their HR-proficient genetic makeup (no biallelic hit in HR-related genes). Not evaluated, no CHORD evaluation because of missing normal reference.

(G–J) The response to the targeted drugs afatinib (G), vemurafenib (H), flavopiridol (I), and adavosertib (J) could partly be explained by genetic aberrations (color-coded) (Tables S6 and S7).

WT, wild-type for the genes mentioned in each panel. NR, IC_{50} value not reached.
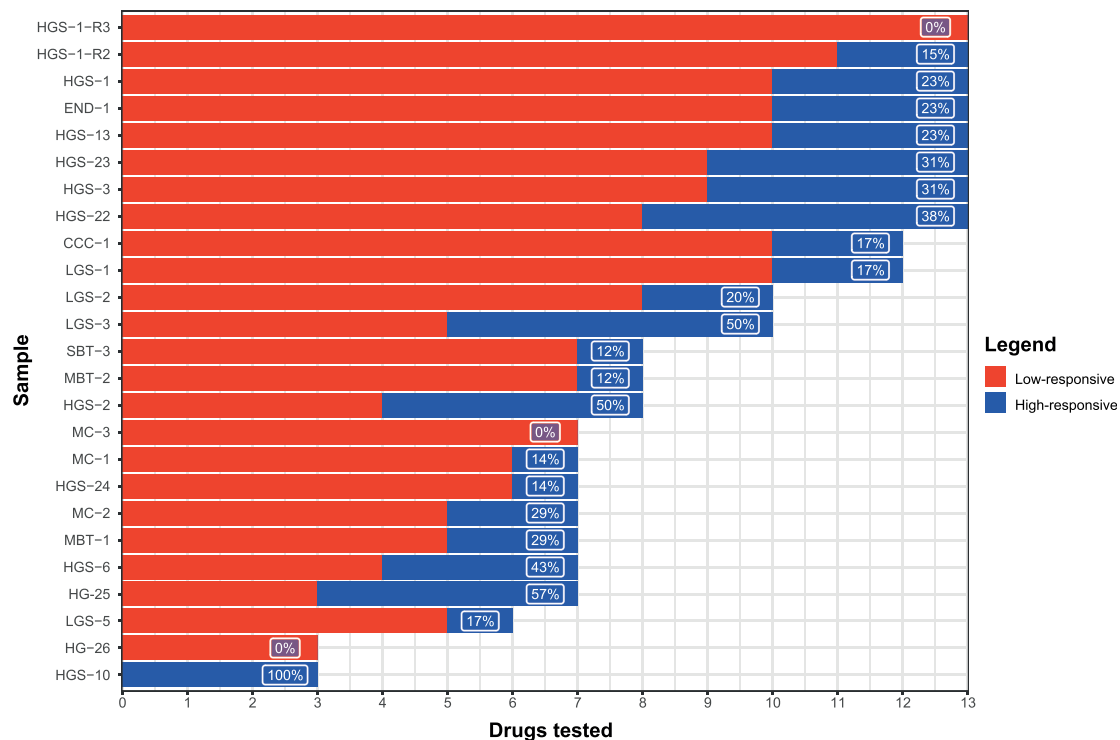
Figure 3. Overview of OC PDO Response to Single Drugs per Patient

Overview of the number of monotherapies tested per patient (3–13), classified as low or high response, based on the IC_{50} value relative to the *in vivo* plasma concentration (C*ss*/C*max*; Table S3). For the majority of patients (88%), high responsiveness to at least one tested drug was identified. For patients with organoids derived from multiple tumor locations, results from all tested samples were considered. Red, low response; blue, high response.

the IC_{50} value of carboplatin and paclitaxel was reduced to 0.56 and −0.34 log μM with combination treatment.

The responses to targeted drugs revealed differences and similarities between PDOs that, in part, correlated with their genetic makeup. For example, all PDOs were classified in the low-response subgroup of the PARP inhibitors olaparib, niraparib, and rucaparib (Figures 2D–2F), consistent with the absence of biallelic inactivation of *BRCA1* and *BRCA2*, and other genes involved in HR (e.g., *CHEK2*, *FANCA*, *PALB2*, *RAD50*, and *RAD51(B/C/D)*; Tables S6 and S7). Additionally, the HR classifier CHORD classified all samples as HR-proficient based on genome-wide somatic mutation contexts (Table S7; Nguyen et al., 2020). As expected, *BRAF*, *KRAS*, and *NRAS* mutant PDOs were classified in the low-response subgroup of the pan-HER inhibitor afatinib (12 of 25; Figure 2G) and high-response subgroup of the BRAF inhibitor vemurafenib (5 of 7; Figure 2H). Alterations in *CDKN2A* and *XIAP*, known to affect response to the CDK inhibitor flavopiridol, were present in our cohort (Cotto et al., 2018; Heilmann et al., 2014; Rosato et al., 2007). *CDKN2A* was affected in the two PDOs that were the least responsive to flavopiridol. MBT-2.1 showed loss of both alleles, and END-1.1 harbored a nonsense variant (p.(R58*); Figure 2I). Copy number loss of *XIAP* was observed in two of the flavopiridol high-response PDOs (Figure 2I). All *TP53* wild-type PDOs (n = 7) were classified into the low-response subgroup of the WEE1 inhibitor adavosertib, whereas *TP53* mutants (n = 15) were distributed among the low- and high-response PDOs (Figure 2J). For

the remaining drugs (alpelisib, AZD-8055, MK-2206, and pictilisib), no known genotype and drug response phenotype correlations were observed.

Subsequently, we evaluated, for each individual patient, how many of the tested monotherapies (3–13 per patient) remained as potential treatments based on an IC_{50} value smaller than the achievable concentration in patient plasma (C*ss*/C*max*). In cases of multiple tumor locations per patient, all test results were considered. A predicted sensitive response (classified in the high-response subgroup) to at least one (and a maximum of five) drug(s) was observed for 88% of patients, except for HGS-1-R3, MC-3, and HG-26, in which all of the 13, seven, and three tested monotherapies yielded a predicted resistant response (classified in the low-response subgroup) in at least one of their PDOs (Figure 3; Table S3).

PDOs Derived from Individual Patients Revealed Intrapatient Drug Response Heterogeneity

In addition to assessing interpatient drug response heterogeneity, we examined intrapatient drug response heterogeneity. For seven individual patients, two to four PDOs were derived from distinct cancer lesions at a single time point. For one additional patient, three PDOs were derived at subsequent time points (Table S1; heterogeneity comparison). To set a threshold for differential drug response, we first assessed the extent of biological variability. We observed low drug response variability across biological replicates (n = 84) with an IC_{50} value correlation

coefficient of $R^2 = 0.82$ and mean IC_{50} fold change of 2.5 ± 1.5 (range = 1.0–7.3) (Figures S3B and S3C; Table S4); therefore, a 10-fold change in IC_{50} value was chosen as a stringent cutoff for differential drug response.

Although homogeneous responses were observed to a subset of drugs and drug combinations (carboplatin combined with gemcitabine, adavosertib, or olaparib, carboplatin, olaparib, niraparib, rucaparib, alpelisib, AZD-8055, flavopiridol, pictilisib, and vemurafenib; Figure S4), all related PDOs exhibited a differential drug response to at least one drug, as defined by a more than 10-fold change in IC_{50} value (Figure 4). In the seven patients from whom multiple PDOs were derived at the same time point, differential response to monotreatment was observed 11 of 36 times (31%). Importantly, in six cases, one of the samples exhibited high responsiveness, whereas a related sample exhibited low responsiveness to the tested drugs.

To examine the effect of intratumor genetic heterogeneity on phenotypic heterogeneity, we assessed genetic variants in genes that are known or predicted to interact with drugs according to the drug-gene interaction database resource (DGIdb; Table S5; Cotto et al., 2018). HGS-13.3, LGS-2.2, LGS-5.2, MC-3.1, and MC-3.2 PDOs were markedly less responsive to the pan-HER inhibitor afatinib compared with their related PDOs, whereas differences in response could not be explained by differences in copy number of EGFR/ERBB2 (HER2)/ERBB3/ERBB4 (Figure 4F; Table S7). Despite meeting the criterion of differential response, all four BRAF mutant LGS-5 PDOs were classified in the low-response subgroup of afatinib with an IC_{50} value above the steady-state concentration of −0.8 log μM. The remaining related PDOs with differential response (HGS-13, LGS-2, and MC-3) were classified in the low- and high-response subgroup of afatinib. We observed differences in KRAS mutation status between the four PDOs derived from a patient with a mucinous OC (MC-3). The two least responsive PDOs (MC-3.1 and MC-3.2) harbored a KRAS hotspot mutation (p.G12V), whereas the other low-response PDO MC-3.4 harbored two different KRAS mutations (p.L19F and p.Q61E, reported to have an attenuated phenotype compared with hotspot mutations; Cooke, 2018; Smith et al., 2010), and the high-response PDO MC-3.3 was KRAS wild-type (WT) (Table S6). KRAS mutations were independently confirmed with Sanger sequencing (Figure S3C).

LGS-5 PDOs also exhibited differential responsiveness to gemcitabine and the MEK inhibitor cobimetinib (Figures 4B and 4G). LGS-5.1 and LGS-5.2 were in the low-response subgroup of gemcitabine, whereas LGS-5.3 and LGS-5.4 were in the high-response subgroup. LGS-5.4 was also highly responsive to cobimetinib, whereas the other LGS-5 PDOs were in the low-response subgroup. All LGS-5 PDOs were largely genetically identical, and no variants or copy number changes were identified that explained the differential response to these drugs (Tables S6 and S7).

HGS-13.3 PDOs revealed a more than 10-fold higher IC_{50} value compared with HGS-13.4 PDOs for gemcitabine, combined carboplatin and paclitaxel treatment, and afatinib (Figures 4B, 4C, and 4F; Table S3). Consistent with previous findings regarding the effect of copper efflux pumps on chemotherapy sensitivity (Nakayama et al., 2002; Samimi et al., 2004a,

2004b), copy number losses of ATP7A and ATP7B were identified in HGS-13.4 (Table S7). Additionally, six other genes previously associated with chemotherapy response (EIF4EBP1, EDNRB, NAT2, TLE3, BRCA2, and NRG1; Del Bufalo et al., 2002; Hegde et al., 2013; Shang et al., 2012) exhibited different copy number states between HGS-13.3 and HGS-13.4, which may also have contributed to the observed differential response to gemcitabine and combined carboplatin and paclitaxel treatment (Table S7).

END-1 PDOs, both derived from distinct parts of the tumor lesion in the same ovary, demonstrated differential drug response to gemcitabine, the WEE1 inhibitor adavosertib, and the AKT inhibitor MK-2206 (Figures 4B, 4D, and 4E). We identified genetic alterations in WWOX, ERBB2, and HRAS that might have contributed to the observed differential response (Tables S6 and S7; Aqeilan et al., 2007; Bunn et al., 2001; Kimura et al., 2006; Liu et al., 2011; Schirmer et al., 2016). However, even though END-1.2 achieved the lowest IC_{50} values for all three drugs, END-1.1 and END-1.2 were classified in the high-response subgroup of gemcitabine and low-response subgroup of MK-2206 and adavosertib (Figures 4B, 4D, and 4E).

HGS-3.1 and LGS-3.1 displayed drug responses that were very similar to their related PDOs (Figure 4; Table S3). In these related PDOs, a differential response was only observed for combined carboplatin and paclitaxel treatment, whereas drug responses were similar to carboplatin and paclitaxel monotreatment. Two carboplatin response-associated genes (Cotto et al., 2018), CLCN6 and MTHFR, exhibited copy number loss in the high-response PDO LGS-3.1 (Table S7). Functional studies have not focused on CLCN6 and chemotherapy response but have shown additive effects of MTHFR inhibition and chemotherapeutic drugs (Stankova et al., 2005).

Additionally, drug response heterogeneity was examined in a patient from whom PDOs were obtained at multiple time points. HGS-1 was derived from primary chemosensitive disease, and HGS-1-R2 and HGS-1-R3 were derived from recurrent chemoresistant disease, and together these PDOs reflected the clinical course of the patient. HGS-1-R2/R3 were less responsive to monotreatment and combination treatment of carboplatin and paclitaxel compared with HGS-1 (Figures 4A and 4C; Table S3). Although HGS-1-R2 and HGS-1-R3 were derived from ascites collected within a time frame of 1 month, differential responsiveness was observed to paclitaxel, gemcitabine, and adavosertib (Figures 4A, 4B, and 4D).

Moreover, we assessed whether structural variants (SVs) (including gene fusions) in genes from the DGIdb resource could be linked to differential drug responses. In the related PDOs derived from the eight patients that exhibited differential drug responses, no SVs were identified that could explain phenotypic heterogeneity. In addition to genetic heterogeneity in genes reported to influence drug response by the DGIdb, related PDOs also exhibited varying degrees of genome-wide heterogeneity at the SNV and CNA levels (Figure 5). The PDOs were sequenced at slightly different passage numbers; therefore, the heterogeneity may also be influenced by tumor content (Table S7) and extended passaging, although we have shown previously that PDOs remained similar at the genomic level after extended passaging (Kopper et al., 2019). The average number of unique
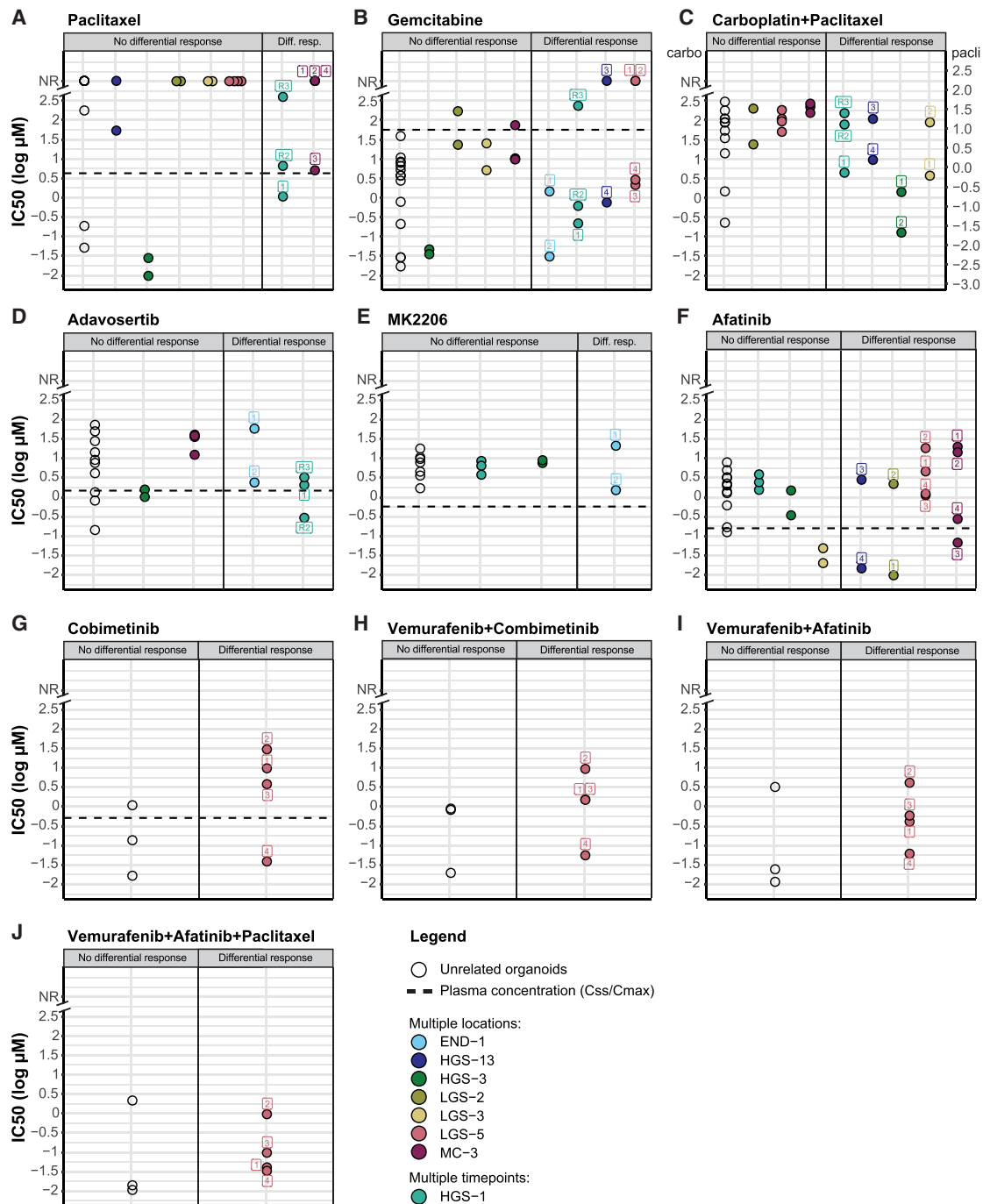
Figure 4. OC PDOs Exhibit Intrapatient Heterogeneity in Response to Chemotherapy and Targeted Drugs

IC_{50} values (extracted from dose-response curves) for drugs that elicit a differential drug response in at least one patient with multiple OC PDOs: paclitaxel (A), gemcitabine (B), carboplatin + paclitaxel (C), adavosertib (D), MK2206 (E), afatinib (F), cobimetinib (G), vemurafenib + cobimetinib (H), vemurafenib + afatinib (I), and vemurafenib + afatinib + paclitaxel (J). Differential drug response is defined as more than 10-fold-change in IC_{50} value within related samples. Left panel: unrelated and related samples without differential response. Right panel: related samples that exhibited differential responses. A color code for each patient is shown. The dotted line indicates the plasma Css or Cmax *in vivo* for all single drug treatments (Table S3).

SNVs and CNAs in all related PDOs were 24% (2%–70%) and 17% (0%–100%), respectively. Considerable genomic heterogeneity at the SNV level was observed in LGS-2 and MC-3

(30%–70% unique SNVs per PDO), whereas these PDOs exhibited differential drug responses to only one/two drugs. On the other hand, END-1 and LGS-5 had the lowest degree of
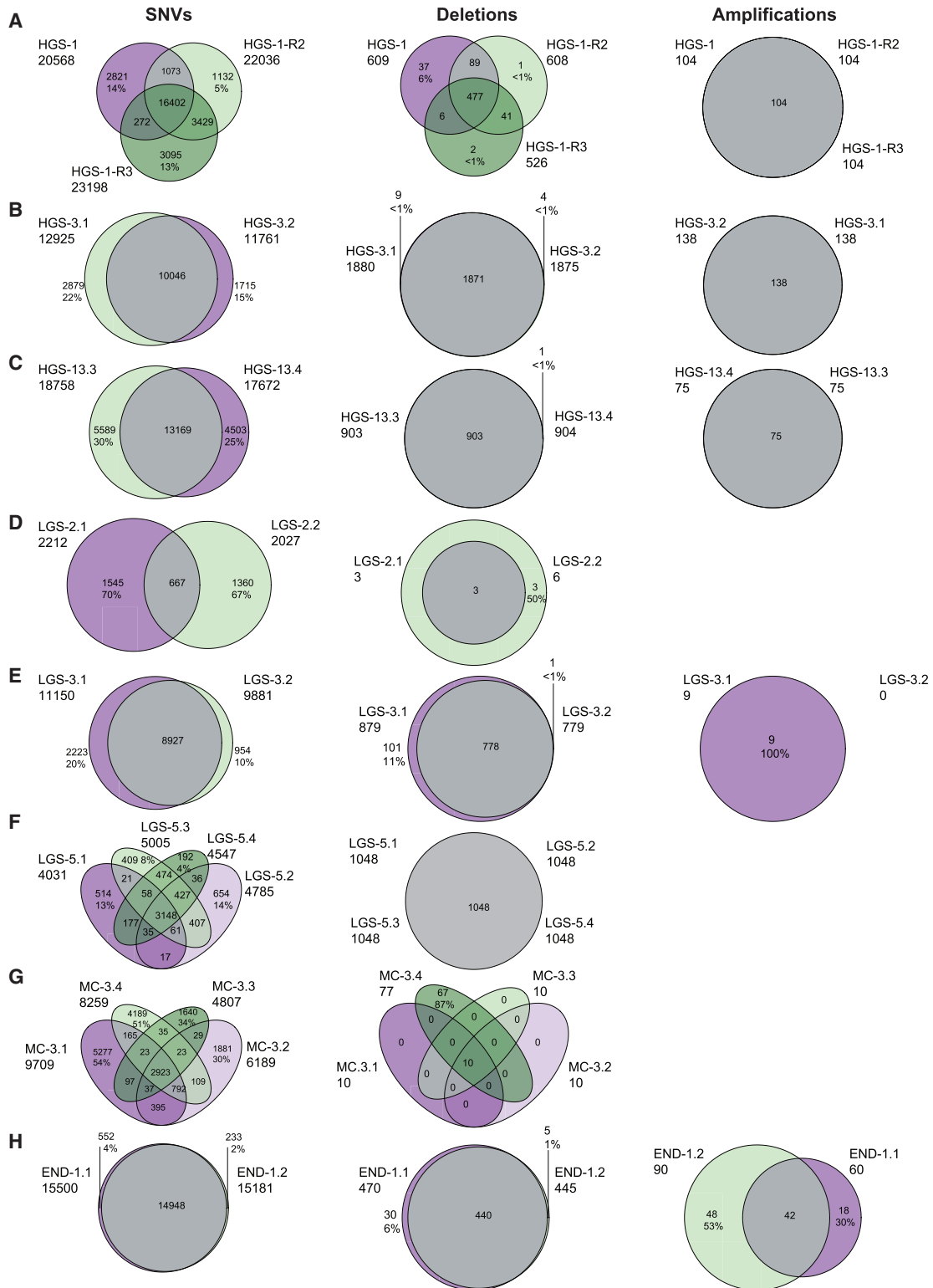
Figure 5. OC PDOs Exhibit Varying Degrees of Genome-wide Heterogeneity at Both the SNV and CNA Level
Venn diagrams showing, from left to right, the overlap of all identified SNVs, deletions, and amplifications among related (A) HGS-1, (B) HGS-3, (C) HGS-13, (D) LGS-2, (E) LGS-3, (F) LGS-5, (G) MC-3, and (H) END-1 OC PDOs. Percentages indicate the unique variants in each PDO.

genomic heterogeneity (2%–14% unique SNVs per PDO) and exhibited a heterogeneous response to three drugs. In conclusion, we did not observe a direct correlation between genome-wide heterogeneity and differential drug response.

DISCUSSION

We performed drug screening on 36 PDOs derived from 23 patients comprising all major OC histopathological subtypes. OC PDOs resembled the tumors from which they were derived, with an average overlap of 67% of SNVs and similar CNA profiles. PDOs generated at interval debulking recapitulated the clinical response to first-line carboplatin and paclitaxel combination treatment for histopathological (p = 5.821e−05), biochemical (p = 0.0004), and radiological (p = 0.0092) outcomes.

Diverse responses to registered drugs for OC were observed among PDOs. Low responsiveness to first-line carboplatin (7 of 31, 23%) and paclitaxel (5 of 31, 16%) treatment was observed compared with high responsiveness in the majority of patients to second-line gemcitabine treatment (29 of 35, 83%). All PDOs exposed to PARP inhibition were found to be low responsive, in line with HR proficiency classification based on whole-genome sequencing (WGS) data. The response to targeted drugs under clinical investigation could be partly explained by genetic variation; low responsiveness to afatinib (12 of 25, 48%), low responsiveness to adavosertib (7 of 17, 41%), high responsiveness to flavopiridol (n = 4 of 17, 24%) and high responsiveness to vemurafenib (5 of 7, 71%). Importantly, we identified a high responsiveness to at least one tested drug in nearly all patients (22 of 25, 88%). Because not all PDOs were exposed to the same number of drugs (3–13 monotherapies tested per patient), this is likely an underrepresentation. Finally, intrapatient tumor heterogeneity assessment in seven patients with organoids derived from multiple tumor locations revealed a differential response to at least one drug for all patients, indicating the importance of evaluating multiple tumor locations.

In a systematic approach, we showed that PDO drug response correlated with several clinical response measures. This included histopathological assessment of tumor regression according to a three-tier method (CRS) (Böhm et al., 2015), which is recommended for assessment of response to neoadjuvant therapy (McCluggage et al., 2015). Histopathological grading of tumor regression offers the advantage to study each tumor site separately, as opposed to patient-wide measures of response, such as CA-125, RECIST, and survival outcomes. Furthermore, it is a direct measure of chemotherapy response, whereas the survival outcomes may also be influenced by completeness of surgery, co-morbidity, and other known prognostic factors. Although Böhm et al. (2015) reported previously that the prognostic significance of the CRS on omental tumor lesions was greater than on primary tumor sites, we applied it to all tumor locations from which organoids were derived. In this study, we present a correlation between CRS and PDO drug response to carboplatin and paclitaxel combination treatment.

To bring PDO-based drug response assessment to the clinic, PDO establishment and drug screening need to be performed within a short time frame, preferably limited to the diagnosis-treatment interval. In line with previous studies (Gotimer et al.,

2019; Hill et al., 2018; Maru et al., 2019; Phan et al., 2019), we demonstrated that PDO establishment and drug screening are feasible within 3 weeks. Other studies showed a time frame of 1–2 weeks. To further validate the predictive value of PDOs, we plan to undertake a prospective trial in which organoids will be derived from primary and recurrent tumors and tested for response to drugs provided in the clinic, whereas clinical response will be systematically monitored.

Considering intrapatient drug response heterogeneity, derivation of organoids from multiple tumor locations of individual patients may further improve treatment allocation (Tiriac et al., 2018). Although sequencing studies have shown that OCs display extensive inter- and intratumor heterogeneity on a genetic level (Hoogstraat et al., 2014; Patch et al., 2015), we could only partially link inter- and intratumor heterogeneous drug responses to genetic heterogeneity. Additionally, some of the CNAs we identified in genes reported to be related to drug response by the DGIdb might be non-contributive passenger events, given the high frequency of CNAs in high-grade serous OC. Therefore, follow-up studies with increased sample sizes and deeper sequencing are required to decipher drug response associations with the candidate genes identified here and to discover novel resistance mechanisms. Importantly however, the lack of complete correlation between genetic and functional testing at this point stresses the need for functional testing in addition to genetic testing to improve clinical decision making.

Establishment of a larger collection of OC PDOs will provide an opportunity to determine comprehensive, clinically useful genotype-phenotype correlations. When a large collection, including drug response data, is available, treatment stratification can potentially be performed based on genomic or transcriptomics characteristics of specific PDO subtypes, which could make organoid derivation dispensable in the future (Tiriac et al., 2018). This transition requires accurate classification of drug-sensitive and -resistant PDOs. Similar to previous studies (Schumacher et al., 2019; Yan et al., 2018), OC PDOs were considered highly responsive when the drug concentration that reduced viability of more than 50% of cells was lower than the concentration achievable in patient plasma (Css/Cmax). However, the Css/Cmax will vary between patients and is not necessarily the concentration that is achieved in the tumor (Pujol et al., 1990; Saleem and Price, 2008). In addition, sometimes patients require dose adjustments because of adverse events that also affect the drug concentration achievable in plasma and tumors. Therefore, it should be taken into account that tumors predicted to be highly responsive based on the PDO drug response may not respond clinically. Prospective clinical trials comparing clinical with PDO drug response, should be complemented with plasma drug level measurements to further elucidate the relation between *in vitro* and clinical responsiveness.

To conclude, OC PDOs provide a valuable preclinical model system to guide treatment choice in the clinic because they satisfy the following criteria: (1) PDOs genetically resemble the original tumor from which they are derived, (2) PDO drug response often reflects patients' clinical response, and (3) PDO establishment and drug screening can be performed within a short time frame. Generating and testing PDOs of

multiple tumor locations will provide insights in differential drug responses as a result of tumor heterogeneity. This information could improve treatment stratification and reduce development of drug resistance. Complementary PDO drug screening and genomic analysis allows linkage of genotypes with drug responsiveness patterns to identify candidate biomarkers for drug response.

STAR★METHODS

Detailed methods are provided in the online version of this paper and include the following:

- KEY RESOURCES TABLE
- RESOURCE AVAILABILITY
  - Lead Contact
  - Materials Availability
  - Data and Code Availability
- EXPERIMENTAL MODEL AND SUBJECT DETAILS
  - Patient samples and clinical data collection
  - Organoid derivation and culture
- METHOD DETAILS
  - *In vitro* PDO drug response testing
  - Clinical drug response measures
  - DNA isolation and whole-genome sequencing
  - WGS data analysis
  - Assessment of homologous recombination status
  - Selection of genes from the DGIdb resource
- QUANTIFICATION AND STATISTICAL ANALYSIS

AUTHOR CONTRIBUTIONS

Conceptualization, C.J.d.W., J.E.V.-I., R.P.Z., P.O.W., and E.S.; Methodology, C.J.d.W., J.E.V.-I., O.K., H.C., W.P.K., and E.S.; Software, J.E.V.-I. and L.N.; Validation, C.J.d.W., N.H., and E.S.; Formal Analysis, C.J.d.W., J.E.V.-I., N.H., C.P.H.V., G.N.J., P.v.D., and E.S.; Investigation, C.J.d.W., N.H., K.L., O.K., and E.S.; Resources, C.J.d.W., J.E.V.-I., K.L., O.K., G.N.J., L.N., R.P.Z., P.O.W., and E.S.; Data Curation, C.J.d.W., J.E.V.-I., and E.S.; Writing – Original Draft, C.J.d.W. and E.S.; Writing – Review & Editing, all authors; Visualization, C.J.d.W., J.E.V.-I., and E.S.; Supervision, W.P.K., E.C., H.J.G.S., R.P.Z., P.O.W., and E.S.; Project Administration, C.J.d.W. and E.S.; Funding Acquisition, H.C., W.P.K., R.P.Z., and P.O.W.

REFERENCES

Aqeilan, R.I., Trapasso, F., Hussain, S., Costinean, S., Marshall, D., Pekarsky, Y., Hagan, J.P., Zanesi, N., Kaou, M., Stein, G.S., et al. (2007). Targeted deletion of Wwox reveals a tumor suppressor function. Proc. Natl. Acad. Sci. USA 104, 3949–3954.

Bleijs, M., van de Wetering, M., Clevers, H., and Drost, J. (2019). Xenograft and organoid model systems in cancer research. EMBO J. 38, e101654.

Boeva, V., Popova, T., Bleakley, K., Chiche, P., Cappo, J., Schleiermacher, G., Janoueix-Lerosey, I., Delattre, O., and Barillot, E. (2012). Control-FREEC: a tool for assessing copy number and allelic content using next-generation sequencing data. Bioinformatics 28, 423–425.

Böhm, S., Faruqi, A., Said, I., Lockley, M., Brockbank, E., Jeyarajah, A., Fitzpatrick, A., Ennis, D., Dowe, T., Santos, J.L., et al. (2015). Chemotherapy Response Score: Development and Validation of a System to Quantify Histopathologic Response to Neoadjuvant Chemotherapy in Tubo-Ovarian High-Grade Serous Carcinoma. J. Clin. Oncol. 33, 2457–2463.

Bunn, P.A., Jr., Helfrich, B., Soriano, A.F., Franklin, W.A., Varella-Garcia, M., Hirsch, F.R., Baron, A., Zeng, C., and Chan, D.C. (2001). Expression of Her-2/neu in human lung cancer cell lines by immunohistochemistry and fluorescence in situ hybridization and its relationship to in vitro cytotoxicity by trastuzumab and chemotherapeutic agents. Clin. Cancer Res. 7, 3239–3250.

Cameron, D.L., Schröder, J., Penington, J.S., Do, H., Molania, R., Dobrovic, A., Speed, T.P., and Papenfuss, A.T. (2017). GRIDSS: sensitive and specific genomic rearrangement detection using positional de Bruijn graph assembly. Genome Res. 27, 2050–2060.

Cameron, D.L., Baber, J., Shale, C., Papenfuss, A.T., Valle-Inclan, J.E., Besselink, N., Cuppen, E., and Priestley, P. (2019). GRIDSS, PURPLE, LINX: Unscrambling the tumor genome via integrated analysis of structural variation and copy number. bioRxiv. https://doi.org/10.1101/781013.

Cingolani, P., Platts, A., Wang, L., Coon, M., Nguyen, T., Wang, L., Land, S.J., Lu, X., and Ruden, D.M. (2012). A program for annotating and predicting the effects of single nucleotide polymorphisms, SnpEff: SNPs in the genome of Drosophila melanogaster strain w1118; iso-2; iso-3. Fly (Austin) 6, 80–92.

Cooke, A. (2018). Biochemical and Biological Characterization of KRAS Q61 Mutants (University of North Carolina at Chapel Hill).

Cotto, K.C., Wagner, A.H., Feng, Y.-Y., Kiwala, S., Coffman, A.C., Spies, G., Wollam, A., Spies, N.C., Griffith, O.L., and Griffith, M. (2018). DGIdb 3.0: a redesign and expansion of the drug-gene interaction database. Nucleic Acids Res. 46 (D1), D1068–D1073.

Del Bufalo, D., Di Castro, V., Biroccio, A., Varmi, M., Salani, D., Rosanò, L., Trisciuoglio, D., Spinella, F., and Bagnato, A. (2002). Endothelin-1 protects ovarian carcinoma cells against paclitaxel-induced apoptosis: requirement for Akt activation. Mol. Pharmacol. 61, 524–532.

Eisenhauer, E.A., Therasse, P., Bogaerts, J., Schwartz, L.H., Sargent, D., Ford, R., Dancey, J., Arbuck, S., Gwyther, S., Mooney, M., et al. (2009). New response evaluation criteria in solid tumours: revised RECIST guideline (version 1.1). Eur. J. Cancer 45, 228–247.

Gotimer, K., Chen, H., Leiserowitz, G.S., and Smith, L.H. (2019). Short-term organoid culture for drug sensitivity testing in high-grade serous ovarian cancer. Gynecol. Oncol. *156*, e27.

Hegde, G.V., de la Cruz, C.C., Chiu, C., Alag, N., Schaefer, G., Crocker, L., Ross, S., Goldenberg, D., Merchant, M., Tien, J., et al. (2013). Blocking NRG1 and other ligand-mediated Her4 signaling enhances the magnitude and duration of the chemotherapeutic response of non-small cell lung cancer. Sci. Transl. Med. *5*, 171ra18.

Heilmann, A.M., Perera, R.M., Ecker, V., Nicolay, B.N., Bardeesy, N., Benes, C.H., and Dyson, N.J. (2014). CDK4/6 and IGF1 receptor inhibitors synergize to suppress the growth of p16INK4A-deficient pancreatic cancers. Cancer Res. *74*, 3947–3958.

Hill, S.J., Decker, B., Roberts, E.A., Horowitz, N.S., Muto, M.G., Worley, M.J., Jr., Feltmate, C.M., Nucci, M.R., Swisher, E.M., Nguyen, H., et al. (2018). Prediction of DNA Repair Inhibitor Response in Short-Term Patient-Derived Ovarian Cancer Organoids. Cancer Discov. *8*, 1404–1421.

Hoogstraat, M., de Pagter, M.S., Cirkel, G.A., van Roosmalen, M.J., Harkins, T.T., Duran, K., Kreeftmeijer, J., Renkens, I., Witteveen, P.O., Lee, C.C., et al. (2014). Genomic and transcriptomic plasticity in treatment-naive ovarian cancer. Genome Res. *24*, 200–211.

Jabs, J., Zickgraf, F.M., Park, J., Wagner, S., Jiang, X., Jechow, K., Kleinheinz, K., Toprak, U.H., Schneider, M.A., Meister, M., et al. (2017). Screening drug effects in patient-derived cancer cells links organoid responses to genome alterations. Mol. Syst. Biol. *13*, 955.

Kimura, K., Sawada, T., Komatsu, M., Inoue, M., Muguruma, K., Nishihara, T., Yamashita, Y., Yamada, N., Ohira, M., and Hirakawa, K. (2006). Antitumor effect of trastuzumab for pancreatic cancer with high HER-2 expression and enhancement of effect by combined therapy with gemcitabine. Clin. Cancer Res. *12*, 4925–4932.

Kopper, O., de Witte, C.J., Lõhmussaar, K., Valle-Inclan, J.E., Hami, N., Kester, L., Balgobind, A.V., Korving, J., Proost, N., Begthel, H., et al. (2019). An organoid platform for ovarian cancer captures intra- and interpatient heterogeneity. Nat. Med. *25*, 838–849.

Li, H., and Durbin, R. (2009). Fast and accurate short read alignment with Burrows-Wheeler transform. Bioinformatics *25*, 1754–1760.

Liu, R., Liu, D., Trink, E., Bojdani, E., Ning, G., and Xing, M. (2011). The Akt-specific inhibitor MK2206 selectively inhibits thyroid cancer cells harboring mutations that can activate the PI3K/Akt pathway. J. Clin. Endocrinol. Metab. *96*, E577–E585.

Maru, Y., Tanaka, N., Itami, M., and Hippo, Y. (2019). Efficient use of patient-derived organoids as a preclinical model for gynecologic tumors. Gynecol. Oncol. *154*, 189–198.

McCluggage, W.G., Judge, M.J., Clarke, B.A., Davidson, B., Gilks, C.B., Hollema, H., Ledermann, J.A., Matias-Guiu, X., Mikami, Y., Stewart, C.J.R., et al.; International Collaboration on Cancer Reporting (2015). Data set for reporting of ovary, fallopian tube and primary peritoneal carcinoma: recommendations from the International Collaboration on Cancer Reporting (ICCR). Mod. Pathol. *28*, 1101–1122.

Mirza, M.R., Monk, B.J., Herrstedt, J., Oza, A.M., Mahner, S., Redondo, A., Fabbro, M., Ledermann, J.A., Lorusso, D., Vergote, I., et al.; ENGOT-OV16/NOVA Investigators (2016). Niraparib Maintenance Therapy in Platinum-Sensitive, Recurrent Ovarian Cancer. N. Engl. J. Med. *375*, 2154–2164.

Nakayama, K., Kanzaki, A., Ogawa, K., Miyazaki, K., Neamati, N., and Takebayashi, Y. (2002). Copper-transporting P-type adenosine triphosphatase (ATP7B) as a cisplatin based chemoresistance marker in ovarian carcinoma: comparative analysis with expression of MDR1, MRP1, MRP2, LRP and BCRP. Int. J. Cancer *101*, 488–495.

Nguyen, L., Martens, J., Van Hoeck, A., and Cuppen, E. (2020). Pan-cancer landscape of homologous recombination deficiency. bioRxiv. https://doi.org/10.1101/2020.01.13.905026.

Ooft, S.N., Weeber, F., Dijkstra, K.K., McLean, C.M., Kaing, S., van Werkhoven, E., Schipper, L., Hoes, L., Vis, D.J., van de Haar, J., et al. (2019). Patient-derived organoids can predict response to chemotherapy in metastatic colorectal cancer patients. Sci. Transl. Med. *11*, eaay2574.

Patch, A.-M., Christie, E.L., Etemadmoghadam, D., Garsed, D.W., George, J., Fereday, S., Nones, K., Cowin, P., Alsop, K., Bailey, P.J., et al.; Australian Ovarian Cancer Study Group (2015). Whole-genome characterization of chemoresistant ovarian cancer. Nature *521*, 489–494.

Phan, N., Hong, J.J., Tofig, B., Mapua, M., Elashoff, D., Moatamed, N.A., Huang, J., Memarzadeh, S., Damoiseaux, R., and Soragni, A. (2019). A simple high-throughput approach identifies actionable drug sensitivities in patient-derived tumor organoids. Commun. Biol. *2*, 78.

Poplin, R., Ruano-Rubio, V., DePristo, M.A., Fennell, T.J., Carneiro, M.O., Van der Auwera, G.A., Kling, D.E., Gauthier, L.D., Levy-Moonshine, A., Roazen, D., et al. (2018). Scaling accurate genetic variant discovery to tens of thousands of samples. bioRxiv. https://doi.org/10.1101/201178.

Priestley, P., Baber, J., Lolkema, M.P., Steeghs, N., de Bruijn, E., Shale, C., Duyvesteyn, K., Haidari, S., van Hoeck, A., Onstenk, W., et al. (2019). Pan-cancer whole-genome analyses of metastatic solid tumours. Nature *575*, 210–216.

Pujol, J.L., Cupissol, D., Gestin-Boyer, C., Bres, J., Serrou, B., and Michel, F.B. (1990). Tumor-tissue and plasma concentrations of platinum during chemotherapy of non-small-cell lung cancer patients. Cancer Chemother. Pharmacol. *27*, 72–75.

Roerink, S.F., Sasaki, N., Lee-Six, H., Young, M.D., Alexandrov, L.B., Behjati, S., Mitchell, T.J., Grossmann, S., Lightfoot, H., Egan, D.A., et al. (2018). Intra-tumour diversification in colorectal cancer at the single-cell level. Nature *556*, 457–462.

Rosato, R.R., Almenara, J.A., Kolla, S.S., Maggio, S.C., Coe, S., Giménez, M.S., Dent, P., and Grant, S. (2007). Mechanism and functional role of XIAP and Mcl-1 down-regulation in flavopiridol/vorinostat antileukemic interactions. Mol. Cancer Ther. *6*, 692–702.

Rustin, G.J.S., Quinn, M., Thigpen, T., du Bois, A., Pujade-Lauraine, E., Jakobsen, A., Eisenhauer, E., Sagae, S., Greven, K., Vergote, I., et al. (2004). Re: New guidelines to evaluate the response to treatment in solid tumors (ovarian cancer). J. Natl. Cancer Inst. *96*, 487–488.

Saleem, A., and Price, P.M. (2008). Early tumor drug pharmacokinetics is influenced by tumor perfusion but not plasma drug exposure. Clin. Cancer Res. *14*, 8184–8190.

Samimi, G., Katano, K., Holzer, A.K., Safaei, R., and Howell, S.B. (2004a). Modulation of the cellular pharmacology of cisplatin and its analogs by the copper exporters ATP7A and ATP7B. Mol. Pharmacol. *66*, 25–32.

Samimi, G., Safaei, R., Katano, K., Holzer, A.K., Rochdi, M., Tomioka, M., Goodman, M., and Howell, S.B. (2004b). Increased expression of the copper efflux transporter ATP7A mediates resistance to cisplatin, carboplatin, and oxaliplatin in ovarian cancer cells. Clin. Cancer Res. *10*, 4661–4669.

Sato, T., Stange, D.E., Ferrante, M., Vries, R.G.J., Van Es, J.H., Van den Brink, S., Van Houdt, W.J., Pronk, A., Van Gorp, J., Siersema, P.D., and Clevers, H. (2011). Long-term expansion of epithelial organoids from human colon, adenoma, adenocarcinoma, and Barrett's epithelium. Gastroenterology *141*, 1762–1772.

Saunders, C.T., Wong, W.S.W., Swamy, S., Becq, J., Murray, L.J., and Cheetham, R.K. (2012). Strelka: accurate somatic small-variant calling from sequenced tumor-normal sample pairs. Bioinformatics *28*, 1811–1817.

Schirmer, M.A., Lüske, C.M., Roppel, S., Schaudinn, A., Zimmer, C., Pflüger, R., Haubrock, M., Rapp, J., Güngör, C., Bockhorn, M., et al. (2016). Relevance of Sp Binding Site Polymorphism in WWOX for Treatment Outcome in Pancreatic Cancer. J. Natl. Cancer Inst. *108*, djv387.

Schumacher, D., Andrieux, G., Boehnke, K., Keil, M., Silvestri, A., Silvestrov, M., Keilholz, U., Haybaeck, J., Erdmann, G., Sachse, C., et al. (2019). Heterogeneous pathway activation and drug response modelled in colorectal-tumor-derived 3D cultures. PLoS Genet. *15*, e1008076.

Shang, Z.-F., Yu, L., Li, B., Tu, W.-Z., Wang, Y., Liu, X.-D., Guan, H., Huang, B., Rang, W.-Q., and Zhou, P.-K. (2012). 4E-BP1 participates in maintaining spindle integrity and genomic stability via interacting with PLK1. Cell Cycle *11*, 3463–3471.

Smith, G., Bounds, R., Wolf, H., Steele, R.J.C., Carey, F.A., and Wolf, C.R. (2010). Activating K-Ras mutations outwit 'hotspot' codons in sporadic colorectal tumours - implications for personalised cancer medicine. Br. J. Cancer *102*, 693–703.

Stankova, J., Shang, J., and Rozen, R. (2005). Antisense inhibition of methylenetetrahydrofolate reductase reduces cancer cell survival in vitro and tumor growth in vivo. Clin. Cancer Res. *11*, 2047–2052.

Swan, H.A., Rosati, R., Bridgwater, C., Churchill, M.J., Watt, R.M., Shaw, R.C., Murphy, S.A., Diaz, R.L., Pereira, S.C., Schaub, F.X., et al. (2018). Abstract 1619: Personalized medicine: A CLIA-certified high-throughput drug screening platform for ovarian cancer. Cancer Res. *78*.

Timmermans, M., Sonke, G.S., Van de Vijver, K.K., van der Aa, M.A., and Kruitwagen, R.F.P.M. (2018). No improvement in long-term survival for epithelial ovarian cancer patients: A population-based study between 1989 and 2014 in the Netherlands. Eur. J. Cancer *88*, 31–37.

Tiriac, H., Belleau, P., Engle, D.D., Plenker, D., Deschênes, A., Somerville, T.D.D., Froeling, F.E.M., Burkhart, R.A., Denroche, R.E., Jang, G.-H., et al. (2018). Organoid Profiling Identifies Common Responders to Chemotherapy in Pancreatic Cancer. Cancer Discov. *8*, 1112–1129.

Vlachogiannis, G., Hedayat, S., Vatsiou, A., Jamin, Y., Fernández-Mateos, J., Khan, K., Lampis, A., Eason, K., Huntingford, I., Burke, R., et al. (2018). Patient-derived organoids model treatment response of metastatic gastrointestinal cancers. Science *359*, 920–926.

Yan, H.H.N., Siu, H.C., Law, S., Ho, S.L., Yue, S.S.K., Tsui, W.Y., Chan, D., Chan, A.S., Ma, S., Lam, K.O., et al. (2018). A Comprehensive Human Gastric Cancer Organoid Biobank Captures Tumor Subtype Heterogeneity and Enables Therapeutic Screening. Cell Stem Cell *23*, 882–897.e11.

STAR★METHODS

KEY RESOURCES TABLE

REAGENT or RESOURCE	SOURCE	IDENTIFIER
Biological Samples		
Human blood reference and ovarian carcinoma tissue samples	Kopper et al., 2019; This study	N/A
Chemicals, Peptides, and Recombinant Proteins		
Advanced DMEM/F12	GIBCO	Cat#12634010
GlutaMAX Supplement	GIBCO	Cat#35050-038
HEPES	GIBCO	Cat#15630-056
Penicillin-Streptomycin	Lonza	Cat#17-602E
Primocin	Bio connect	Cat#ant-pm-1
R-spondin conditioned medium	In-house production	N/A
Noggin conditioned medium	In-house production	N/A
WNT conditioned medium	In-house production	N/A
B-27 Supplement	Life technologies	Cat#17504001
Nicotinamide	Sigma	Cat#N0636
N-Acetyl-L-cysteine	Sigma	Cat#A9165
Hydrocortisone	Sigma	Cat#H0888
Heregulinβ-1 human recombinant	Peprotech	cat#100-03
FGF10 human recombinant	Peprotech	Cat#100-26
EGF human recombinant	Peprotech	Cat#AF-100-15
Forskolin	TOCRIS	Cat#1099
A83-01	R&D systems	Cat#2939/10
Y-27632 Dihydrochloride (RhoKi)	Gentaur	Cat#A3008
β-Estradiol	Sigma	Cat#E2257
Collagenase	Sigma	Cat#C9407
Red blood cell lysis buffer	Roche	Cat#11814389001
Dispase II	GIBCO	Cat#1710541
Recovery Cell Culture Freezing Medium	GIBCO	Cat#12648010
Cell titer Glo 2.0	Promega	Cat#G9243
BME (Cultrex growth factor reduced BME type 2)	Amsbio	N/A
Alpelisib (BYL719)	Selleckchem	Cat#S2814
Adavosertib (MK-1775)	Selleckchem	Cat#S1525
Afatinib (BIBW2992)	Selleckchem	Cat#S1011
AZD8055	Selleckchem	Cat#S1555
Carboplatin	Selleckchem	Cat#S1215
Gemcitabine	Selleckchem	Cat#S1714
MK-2206	Selleckchem	Cat#S1078
Niraparib (MK-4827)	Selleckchem	Cat#S2741
Olaparib (AZD2281, Ku-0059436)	Selleckchem	Cat#S1060
Paclitaxel	Selleckchem	Cat#S1150
Pictilisib (GDC-0941)	Selleckchem	Cat#S1065
Rucaparib (AG-014699,PF-01367338)	Selleckchem	Cat#S1098
Vemurafenib (PLX4032, RG7204)	Selleckchem	Cat#S1267
Flavopiridol (146426-40-6)	Bio connect	Cat#HY-10005

(Continued on next page)

Continued

REAGENT or RESOURCE	SOURCE	IDENTIFIER
Cobimetinib (GDC-0973)	Active Biochem	Cat#A-1180
QIAGEN Proteinase K	QIAGEN	Cat#19133
RNase A	QIAGEN	Cat#19101
Critical Commercial Assays		
Dneasy blood en tissue kit	QIAGEN	Cat#69504
Genomic Tip 100/G kit	QIAGEN	Cat#10243
Genomic DNA Buffer Set	QIAGEN	Cat#19060
Deposited Data		
Whole-genome sequencing	This study	EGAD00001005707
Experimental Models: Organoids		
Human ovarian cancer organoids	Kopper et al., 2019; This study	https://huborganoids.nl/
Oligonucleotides		
KRAS Fw-TTTTTGAAGTAAAAGGTGCACTG	This study	N/A
KRAS Rv-CATGAAAATGGTCAGAGAAACC	This study	N/A
Software and Algorithms		
Graphpad prism 6	Graphpad	https://www.graphpad.com/scientific-software/prism/
R-studio version 3.5.0	R	https://rstudio.com/
Custom code	This study	https://github.com/UMCUGenetics/OvCa_organoids_heterogeneity
Hartwig Medical Foundation WGS cancer analysis pipeline (v4.8)	Hartwig Medical Foundation; Priestley et al., 2019	https://github.com/hartwigmedical/pipeline; https://github.com/UMCUGenetics/guix-additions
BWA-MEM (v0.7.5a)	Li and Durbin, 2009	https://github.com/lh3/bwa
Genome Analysis Toolkit (GATK, v3.8.1)	Poplin et al., 2018	https://gatk.broadinstitute.org/hc
Strelka (v1.0.14)	Saunders et al., 2012	https://github.com/Illumina/strelka
SnpEff (v4.3)	Cingolani et al., 2012	http://snpeff.sourceforge.net/
GRIDSS (v1.8.0)	Cameron et al., 2017	https://github.com/PapenfussLab/gridss
PURPLE (v2.17)	Cameron et al., 2019	https://github.com/hartwigmedical/hmftools/tree/master/purity-ploidy-estimator
Control-FREEC (v. 11.0)	Boeva et al., 2012	http://boevalab.inf.ethz.ch/FREEC/
ClinVar (GRCh37, database date 2018-12-07)	NIH	https://www.ncbi.nlm.nih.gov/clinvar/
CHORD (v1.04)	Nguyen et al., 2020	https://github.com/UMCUGenetics/CHORD
Other		
Whole-genome sequencing	Kopper et al., 2019	EGAD00001004387
Drug Gene Interaction database 3.0	Cotto et al., 2018	http://dgidb.org/ Accessed on 26-08-2019

RESOURCE AVAILABILITY

Lead Contact

Further information and requests for resources and reagents should be directed to and will be fulfilled by the Lead Contact, Ellen Stelloo (estelloo@umcutrecht.nl).

Materials Availability

Available OC PDOs are cataloged at https://huborganoids.nl/ and can be requested at info@hub4organoids.eu. Distribution of OC PDOs to third parties will have to be authorized by the IRB UMCU at the request of the HUB to ensure compliance with the Dutch 'medical research involving human subjects' act.

Data and Code Availability

BAM files of whole-genome sequencing data are made available through controlled access at the European Genome-phenome Archive (EGA) which is hosted at the EBI and the CRG (https://ega-archive.org). The accession number for the sequencing data reported in this paper is EGA: EGAD00001005707. The accession number for the sequencing data reported in Kopper et al., 2019 is EGA: EGAD00001004387. Data access requests will be evaluated by the UMCU Department of Genetics Data Access Board (EGAC00001000432) and transferred on completion of a material transfer agreement and authorization by the IRB UMCU at the request of the HUB to ensure compliance with the Dutch 'medical research involving human subjects' act. Additionally, custom code for genomic analyses is available in https://github.com/UMCUGenetics/OvCa_organoids_heterogeneity.

EXPERIMENTAL MODEL AND SUBJECT DETAILS

Patient samples and clinical data collection

For this study we included women diagnosed with epithelial OC (median age: 65 years). Each patient signed informed consent and was able to withdraw her consent at any time. Tumor samples, ascites and blood samples were gathered between January 2016 and September 2019 at the University Medical Center Utrecht, and Leiden University Medical Center, the Netherlands. Patient data and tissue collection was performed according to the guidelines of the European Network of Research Ethics Committees (EUREC) following European, national and local law. The Institutional Review Board of the UMC Utrecht (IRB UMCU) approved the biobanking protocol: 14-472 HUB-OVI. Clinical data was collected from the patient files. Patient samples were derived at primary disease during primary debulking surgery or interval debulking surgery, or adnex extirpation procedures. Upon recurrence, tissue was collected during (laparoscopic) surgery performed for treatment or diagnostic purposes, or ascites was collected during palliative drainage procedures. No statistical test was used to predetermine sample size.

For the clinical-PDO drug response comparison we selected the samples that met all of the following three conditions: 1) samples were derived at intervaldebulking surgery; 2) organoid drug response data to carboplatin/paclitaxel was available; 3) patient drug response to carboplatin/paclitaxel was available. For the intrapatient heterogeneity comparison we selected all patients of whom multiple PDOs were derived.

Organoid derivation and culture

Organoids were derived from tumor samples of patients with OC and cultured according to our previously described protocol (Kopper et al., 2019). Briefly, tumor tissue was cut into small pieces. Two random pieces were separated for fixation in formalin for histopathological analysis and DNA isolation. The remaining tissue was minced, washed with 10 ml advanced DMEM/F12 containing 1x Glutamax, 10 mM HEPES and antibiotics (AdDF+++), collected in a tube, and centrifuged at 300 g for 5 minutes. Fragments were allowed to settle under normal gravity for 1 minute, and remaining big tissue pieces were digested in AdDF+++ supplemented with 5 μM RHO/ROCK pathway inhibitor (Y-27632) containing 0.5–1.0 mg/ml collagenase at 37 °C for 0.5–1.0 h. Ascites/pleural effusion samples were centrifuged, and washed with AdDF+++. The cell pellet was allocated fixation in formalin, DNA isolation and organoid derivation. To eliminate erythrocytes, the samples for organoid derivation were incubated with 2 ml red blood cell lysis buffer for 5 min at room temperature followed by an additional wash with 10 ml AdDF+++ and centrifugation at 300 g for 5 minutes. Finally, the cells were embedded in BME (Cultrex growth factor reduced BME type 2) on ice and seeded on pre-warmed 24-well suspension culture plates. Following BME polymerization, the cells were overlaid with appropriate organoid culture medium and incubated at 37°C in humidified air containing 5% CO2 (see Table S1). PDO names are informative of histological subtype, patient and tumor location. Histological subtype: HGS/LGS = high/low-grade serous adenocarcinoma, HG = high-grade adenocarcinoma, SBT/MBT = serous/mucinous borderline tumor, MC = mucinous adenocarcinoma, CCC = clear cell carcinoma, END = endometrioid carcinoma. The first number indicates the patient, the second number indicates tumor location.

METHOD DETAILS

In vitro PDO drug response testing

PDO drug response testing was performed as previously described (Kopper et al., 2019). In short, PDOs were exposed to drugs in varying concentrations and to controls (DMSO, ABT-263/navitoclax) for 120 hours in 384-well plates, after which ATP levels were measured with the Cell-Titer Glo2.0 assay. All screens were performed in technical replicates. Biological replicates were performed in a subset of PDOs and drugs (Table S4) to investigate biological variation. Results were normalized to vehicle (DMSO = 100%) and baseline control (ABT-263/navitoclax 20 μM). Data were analyzed using GraphPad Prism 6. Drug dose-response curves were visualized using linear regression analysis (setting: log(inhibitor) versus response; least-squares (ordinary) fit; top constraint 100%). Concentrations where 50% cell viability (IC$_{50}$-value) was reached were interpolated. The area under the curve (AUC) was approximated between the lowest and highest concentrations screened in the actual assay with the trapezoid rule for numerical integration.

Clinical drug response measures

Histopathological response was assessed with the chemotherapy response score (CRS) after three cycles of neoadjuvant chemotherapy, according to the guidelines described by Böhm et al. (2015). All available hematoxylin and eosin stained slides of each tumor

location from which we established PDOs were assessed for tumor purity. The slide with the most tumor per location was subsequently blinded scored by two certified pathologists (PvD, CV), as CRS-1 (no or minimal pathological response), CRS-2 (appreciable pathological response) or CRS-3 (complete or near-complete pathological response). In case of disagreement consensus was reached. Radiological response was assessed according to the RECIST criteria for solid tumors (version 1.1) (Eisenhauer et al., 2009). A score for each patient was obtained, from best to worst response: complete response (CR), partial response (PR), stable disease (SD), or progressive disease (PD). Biochemical response was measured by assessing response and timing of normalization (< 35kU/L) of biomarker cancer antigen 125 (CA-125) (Rustin et al., 2004). For progression-free survival (PFS) a cut-off of six months was employed; since patients with less than six months PFS are predicted to be resistant to subsequent platinum-treatment. For overall survival, 17 months was taken as a cut-off, based on survival data of a recent cohort of patients (2015-2016) with HGS OC stage IV disease by the Dutch Cancer Registration. Seventeen months after diagnosis, 50% of patients with HGS OC stage IV were still alive.

DNA isolation and whole-genome sequencing
DNA was isolated with the DNeasy QIAGEN kit (PDOs and blood samples) and Genomic Tip QIAGEN kit (tumor samples), supplemented with RNase treatment. Fresh frozen tumor material obtained through biopsy procedures was processed with the QiaSymphony DSP DNA kit for low input. For DNA library preparation, 500–1,000 ng of DNA was used. Subsequently, whole-genome paired-end sequencing (WGS; 2x 150 bp) was performed on Illumina HiSeq X Ten and NovaSeq 6000 to a median coverage of 31X (range 24-45X).

WGS data analysis
WGS data were processed using the Hartwig Medical Foundation (HMF) somatic mutation workflow. We installed the pipeline (v4.8) locally using GNU Guix with the recipe from https://github.com/UMCUGenetics/guix-additions. Full details and pipeline description are explained in detail by Priestley et al. (2019) (https://github.com/hartwigmedical/pipeline). Briefly, sequence reads were mapped against human reference genome GRCh37 with Burrows-Wheeler Alignment (BWA-MEM) (v0.7.5a) (Li and Durbin, 2009). Indel realignment and base recalibration was performed with the Genome Analysis Toolkit (GATK, v3.8.1) (Poplin et al., 2018). Somatic single nucleotide variants (SNVs) and small insertions and deletions were called with Strelka (v1.0.14) (Saunders et al., 2012). The functional effect of the somatic SNVs and indels were predicted with SnpEff (v.4.3) (Cingolani et al., 2012). Somatic structural variants (SVs) were called with GRIDSS (v1.8.0) (Cameron et al., 2017). To assess the SNV overlap between an organoid and a corresponding tumor sample, SNVs that were only detected in either the tumor or the organoid sample of a pair were in a subsequent step called in the corresponding sample (tumor or organoid) when supported by at least one read.

Copy number alterations (CNAs) were called with PURPLE (v2.17) (Cameron et al., 2019). PURPLE also assesses tumor purity. In case of low tumor purity, a "NO_TUMOR" quality flag was raised by PURPLE, meaning PURPLE failed to find any aneuploidy, and somatic variants were supplied but there were fewer than 300 with observed VAF > 0.1, indicating a high normal cell content (Table S7). For tumor samples MC-3.2, MC-3.3, MBT-2.1 and MC-1.2, based on manual verification, a wrong ploidy level was automatically selected by PURPLE. We verified with metaphase spreads analysis on MC-3.2, MBT-2.1 and MC-1.2 PDOs that a ploidy of 2 was most likely for those PDOs and tumor samples. Therefore, and due to the impossibility of manually correcting the ploidy selection in PURPLE, we ran Control-FREEC (v. 11.0) (Boeva et al., 2012) instead on all samples (tumor and PDO) from those patients. Telomeric and centromeric regions were masked for visualization.

For samples CCC-1, END-1.1, END-1.2, HGS-22 and HGS-23 no normal reference sample was available for somatic mutation calling. In these cases, germline SNV calling was performed with GATK (Poplin et al., 2018) and only SNVs with a "HIGH" or "MODERATE" effect as predicted by SnpEff were considered. Similarly, germline SV calling was performed using GRIDSS and SV calls were filtered against the SV Panel of Normals from the HMF analysis pipeline, which can be found in https://nextcloud.hartwigmedicalfoundation.nl/s/LTiKTd8XxBqwaiC. Since PURPLE requires tumor-normal pairs, CNA calling for these five samples was performed individually with Control-FREEC (v. 11.0) (Boeva et al., 2012).

Assessment of homologous recombination status
To identify homologous recombination (HR)-deficient samples, *BRCA1* and *BRCA2* as well as other genes in the HR-pathway (*BARD1, BRIP1, CHEK2, FANCA, PALB2, RAD50, RAD51(B/C/D)*) were assessed for biallelic inactivation, incorporating both germline and somatic WGS data. Biallelic inactivation was defined as: a deep deletion (i.e., full loss of both alleles); or Loss-Of-Heterozygosity (LOH) in combination with (i) a known pathogenic/likely pathogenic variant according to ClinVar (https://www.ncbi.nlm.nih.gov/clinvar/; GRCh37, database date 2018-12-07), or (ii) a frameshift, nonsense or essential splice variant as annotated by SnpEff (http://snpeff.sourceforge.net; v4.1h). Additionally, CHORD (**C**lassifier of **HO**mologous **R**ecombination **D**eficiency, v1.04) was employed to classify PDO samples as HR-proficient or -deficient based on the presence of genome-wide somatic mutation contexts (primarily deletions with flanking microhomology and 1-100kb structural duplications) (Nguyen et al., 2020). Samples without a germline reference sample were excluded from CHORD evaluation.

Selection of genes from the DGIdb resource

The Drug Gene Interaction database (DGIdb) was utilized as a resource to obtain a list of genes that have a known interaction with drug response (Cotto et al., 2018). WGS data of PDOs were checked for SNVs, SVs and CNAs in DGIdb genes, in case differential drug response was observed within related PDOs. Homo-polymer regions were excluded. To identify significantly amplified and deleted genes we applied stringent criteria adopted from Priestley et al. (2019). An amplification was defined as [minimum exonic copy number > three times the sample ploidy], while a deletion was defined as [minimum exonic copy number < 0.5 times the sample ploidy]. Related samples were regarded genetically heterogeneous on copy number level, if they presented with different copy-number states (amplified versus neutral versus deleted). Furthermore, differential response among related samples was only considered if the ploidy-corrected copy number levels were > 10% apart.

QUANTIFICATION AND STATISTICAL ANALYSIS

Descriptive statistics including mean, SD and SEM were conducted with R or GraphPad Prism. The significance level for 95% confidence interval was set to $\alpha = 0.05$. The Pearson correlation test was applied to evaluate the correlation between replicate experiments. The Wilcoxon signed-rank test was applied for the comparison of clinical response groups. The means of two technical replicates of each sample at all measured drug concentrations were compared between clinical response groups (CRS-1 versus −2, RECIST SD versus PR, no CA-125 normalization versus normalization, PFS < 6 months versus > = 6 months, OS < 17 months versus > = 17 months). We corrected for multiple testing with the Bonferroni method (alpha = 0.05 / 5 (tests)), resulting in a statistically significant threshold of p = 0.01.